2018 IEEE Conference on Decision and Control (CDC)
Miami Beach, FL, USA, Dec. 17-19, 2018

Conditions for Delay-Robust Consensus-Based Frequency Control in Power Systems with Second-Order Turbine-Governor Dynamics

Sultan Alghamdi, Johannes Schiffer, Emilia Fridman

Abstract— **Consensus-based distributed secondary frequency control schemes have the potential to simultaneously ensure real-time frequency restoration and economic dispatch in future power systems with large shares of renewable energy sources. Yet, due to their distributed nature these control schemes critically depend on communication between units and, thus, robustness with respect to communication uncertainties is crucial for their reliable operation. Furthermore, when applied in bulk power systems the control design and analysis should take higher-order turbine-governor dynamics of the generation units explicitly into account. Both aspects have not been addressed jointly in the existing literature. Motivated by this, we derive conditions for robust stability of a consensus-based distributed frequency control scheme applied to a power system model with second-order turbine-governor dynamics in the presence of heterogeneous time-varying communication delays and dynamic communication topology. The result is established by a novel coordinate transformation and reduction to eliminate the invariant subspace in the closed-loop dynamics and by constructing a strict common Lyapunov-Krasovskii functional.**

I. Introduction

A. Motivation and Related Work

Maintaining a reliable and efficient operation of large scale power systems is becoming increasingly challenging due to the high penetration of renewable energy resources (RES) [1]. The latter lead to higher and faster varying power imbalances. As a result of any imbalance between generation and demand, the frequency deviates from its nominal value [2]. Therefore, one of the most critical control challenges in power systems is frequency regulation. Conventionally, frequency regulation is carried out via three hierarchical control layers: primary, secondary and tertiary control [2]. The primary layer is a proportional control that acts fast on the instantaneous frequency deviation in a fully decentralized manner. The secondary control action is usually deployed via a centralized automatic generation control (AGC). Furthermore, tertiary control is mainly concerned with energy management.

However, the rising volatility in RES infeed and the accompanying uncertainty makes centralized operation schemes increasingly inappropriate to provide the flexibility required to secure a stable network operation [1]. As a consequence, distributed secondary frequency control schemes seeking to combine frequency regulation with optimal generation dispatch in real-time have recently attracted significant attention. Essentially, the available concepts can be classified into two groups: primal-dual gradient-based algorithms [3]–[5] and consensus-based approaches [6]–[10]. The main advantages of primal-dual approaches are that generic convex cost functions and capacity constraints can be considered in the design. Yet, a key drawback is that exact information on the actual load demand needs to be available, which is a stringent requirement in practice (see also the discussion in [3]). Compared to this, consensus-based algorithms only admit quadratic cost functions. Yet, they have the fundamental advantage that merely local frequency measurements and information exchange of the control variable are required and are, hence, significantly simpler to implement.

Most existing results for stability of consensus-based frequency controllers are limited to generator dynamics modeled by the swing equation and assume ideal communication [6]–[8]. Exceptions are [9], [10] in which higher-order turbine-governor dynamics are considered and [11], [12] in which the impact of communication uncertainties on the control performance is analysed. The latter is of paramount importance, since any distributed control scheme relies on information exchange between generators. Thus, guaranteeing robustness with respect to communication uncertainties, such as delays, message losses and link failures [13], [14], is essential to further promote a practical implementation of consensus-based control schemes in power systems. For the same reason, more realistic generator models need to be considered. We remark that the inclusion of second-order turbine governor dynamics is used in many related stability studies on classical AGC [15]–[20].

B. Contributions

In light of the above facts, the main contribution of the present paper is the derivation of sufficient delay-dependent conditions which guarantee robust stability of higher-order power system dynamics equipped with a consensus-based secondary frequency control scheme. Compared to existing work [9]–[11], we simultaneously account for second-order turbine-governor dynamics as well as time-varying communication uncertainties. Following [21]–[25], the latter are represented by heterogeneous fast-varying delays together with a dynamic communication network. The presence of higher-order (non-passive) and time-varying dynamics significantly complicates the stability analysis. However, if not accounted

S. Alghamdi and J. Schiffer are with School of Electronic & Electrical Engineering, University of Leeds, United Kingdom, LS2 9JT {elsalg,j.schiffer}@leeds.ac.uk

E. Fridman is with Tel-Aviv University, Israel emilia@eng.tau.ac.il

This work was partially supported by the Engineering and Physical Sciences Research Council (EPSRC) [grant number EP/R030243/1]. J. Schiffer acknowledges funding from the European Union's Horizon 2020 research and innovation programme under the Marie Skłodowska-Curie grant agreement No. 734832.

for in the analysis their presence may lead to instability, see, e.g., the example showing instability for power systems with non-passive second-order turbine governor dynamics in [9]. To cope with these challenges, we derive a suitable coordinate transformation and reduction to eliminate the invariant subspace introduced in the closed-loop dynamics by the consensus-based control. Furthermore, unlike the Lyapunov functions employed in [9], [10], our result is established by constructing a *strict* common Lyapunov-Krasovskii functional (LKF) for the nonlinear higher-order power system dynamics. The effectiveness of the derived conditions is illustrated via a numerical example.

The remainder of this paper is structured as follows. In Section II, we recall some preliminaries on graph theory, power network modeling, optimal consensus-based frequency control and communication uncertainties. The robust stability analysis based on a strict LKF is presented in III. A numerical example to demonstrate the effectiveness of the approach is given in Section IV. A brief summary and topics of future work are provided in Section V.

Notation. We define the sets $\mathbb{R}_{\geq 0} := \{x \in \mathbb{R} | x \geq 0\}$, $\mathbb{R}_{>0} := \{x \in \mathbb{R} | x > 0\}$ and $\mathbb{R}_{<0} := \{x \in \mathbb{R} | x < 0\}$, $\mathbb{Z}_{\geq 0} := \{0, 1, 2, \ldots\}$. For a set $\mathcal{V}$, $|\mathcal{V}|$ denotes its cardinality and $[\mathcal{V}]^k$ denotes the set of all subsets of $\mathcal{V}$ that contain k elements. Let $x := \text{col}(x_i) \in \mathbb{R}^n$ denote a vector with entries x_i for $i = 1, \ldots, n$, $\mathbb{1}_n$ the vector with all entries equal to one, I_n the $n \times n$ identity matrix, $\text{diag}(a_i), i = 1, \ldots, n$ an $n \times n$ diagonal matrix with diagonal entries $a_i \in \mathbb{R}$ and $A = \text{blkdiag}(A_i)$ denotes a block-diagonal matrix with block-diagonal matrix entries A_i. Moreover, $\mathbb{0}$ denotes a quadratic zero matrix of appropriate dimensions. For non-quadratic zero matrices the dimensions are specified, i.e., $\mathbb{0}_{n \times m}$ with $m \neq n$. For $A \in \mathbb{R}^{n \times n}$, $A > 0$ ($A < 0$) means that A is symmetric positive (negative) definite. The lower-diagonal elements of a symmetric matrix are denoted by $*$. We denote by $W[-h, 0]$, $h \in \mathbb{R}_{>0}$, the Banach space of absolutely continuous functions $\phi : [-h, 0] \to \mathbb{R}^n$, $h \in \mathbb{R}_{>0}$, with $\dot{\phi} \in L_2(-h, 0)^n$ and with the norm $\|\phi\|_W = \max_{\theta \in [a,b]} |\phi(\theta)| + \left(\int_{-h}^{0} \dot{\phi}^2 d\theta \right)^{0.5}$. Also, ∇f denotes the gradient of a function $f : \mathbb{R}^n \to \mathbb{R}$.

II. Preliminaries

A. Algebraic Graph Theory

An undirected graph of order n is a tuple $\mathcal{G} = (\mathcal{V}, \mathcal{E})$ with set of nodes $\mathcal{V} = \{1, \ldots, n\}$ and set of undirected edges $\mathcal{E} \subseteq [\mathcal{V}]^2$, $\mathcal{E} = \{e_1, \ldots, e_m\}$, $m = |\mathcal{E}|$. The entries of the adjacency matrix $\mathcal{A} \in \mathbb{R}^{|\mathcal{N}| \times |\mathcal{N}|}$ are defined as $a_{ik} = 1$ if there is an edge between nodes i and k and $a_{ik} = 0$ otherwise. The degree of a node is given by $d_i = \sum_{k=1}^{|\mathcal{N}|} a_{ik}$. With $\mathcal{D} = \text{diag}(d_i) \in \mathbb{R}^{|\mathcal{N}| \times |\mathcal{N}|}$, the Laplacian matrix of an undirected graph is defined as $\mathcal{L} = \mathcal{D} - \mathcal{A}$. An ordered sequence of nodes such that any pair of consecutive nodes in the sequence is connected by an edge is called a path. A graph $\mathcal{G}$ is said to be connected if for all pairs $\{i, k\} \in [\mathcal{V}]^2$ there exists a path from i to k. The Laplacian matrix $\mathcal{L}$ of an undirected graph is positive semidefinite with a simple zero eigenvalue if and only if the graph is connected. The corresponding right eigenvector to this simple zero eigenvalue is $\mathbb{1}_n$, i.e., $\mathcal{L}\mathbb{1}_n = \mathbb{0}_n$ [26]. We refer the reader to [26], [27] for further information on graph theory.

B. Power Network Model with Second-Order Turbine-Governor Dynamics

We consider a Kron-reduced power system model with $n \geq 1$ nodes and denote the set of nodes by $\mathcal{N} = \{1, \cdots, n\}$. We assume that at each node a generator is connected and assign a phase angle $\theta_i : \mathbb{R}_{\geq 0} \to \mathbb{R}$ and relative frequency $\omega_i = \dot{\theta}_i - \omega^d$, where $\omega^d \in \mathbb{R}_{\geq 0}$ is the desired (nominal) network frequency, to each unit $i \in \mathcal{N}$. It is convenient to define the vectors $\theta = \text{col}(\theta_i)$ and $\omega = \text{col}(\omega_i)$. Moreover, we make the following standard assumptions: the voltage amplitudes $V \in \mathbb{R}^n_{\geq 0}$ are positive constants and the line impedances are purely inductive [2]. Under the previous assumptions, two nodes i and k are connected via a nonzero susceptance $B_{ik} \in \mathbb{R}_{<0}$. Thus, $B_{ik} = 0$ if there is no connection between i and k. Furthermore, we assume that for all $\{i, k\} \in [\mathcal{N}]^2$ there exists an ordered sequence of nodes from i to k such that any pair of consecutive nodes in the sequence is connected by a power line represented by an admittance, i.e., the electrical network is connected. The active power flow can be written as follows $P : \mathbb{R}^n \to \mathbb{R}^n$,

$$P(\theta) = \nabla U(\theta),$$

where the potential function $U : \mathbb{R}^n \to \mathbb{R}$ is given by

$$U(\theta) = - \sum_{\{i,k\} \in [\mathcal{N}]^2} |B_{ik}| V_i V_k \cos(\theta_{ik}).$$

Moreover, different from the analysis in [11], [12], we consider a more realistic higher-order generator model with second-order turbine-governor dynamics given by [28, Chapter 4]

$$\begin{aligned} \dot{\theta} &= \omega, \\ M\dot{\omega} &= -D\omega - \nabla U(\theta) - GV^2 + P_m^d + P_m, \\ T_m \dot{P}_m &= -P_m + P_s, \\ T_s \dot{P}_s &= -P_s - K^{-1}\omega + p, \end{aligned} \tag{II.1}$$

where $P_m : \mathbb{R}_{\geq 0} \to \mathbb{R}^n$ is the mechanical power, $P_s : \mathbb{R}_{\geq 0} \to \mathbb{R}^n$ is the steam power and $p : \mathbb{R}_{\geq 0} \to \mathbb{R}^n$ is the secondary control signal. Furthermore, the diagonal and positive definite matrices $D \in \mathbb{R}^{n \times n}$, $M \in \mathbb{R}^{n \times n}$, $K \in \mathbb{R}^{n \times n}$, $T_m \in \mathbb{R}^{n \times n}$ and $T_s \in \mathbb{R}^{n \times n}$ denote the damping coefficients, inertia coefficients, droop gains, governor time constants and turbine time constants, respectively. In addition, GV^2 represents the active power demand, where $G = \text{col}(G_{ii}) \in \mathbb{R}^n_{\geq 0}$ and $G_{ii} \in \mathbb{R}_{\geq 0}$ is the shunt conductance at the i-th node, and $P_m^d \in \mathbb{R}^n_{\geq 0}$ denotes the vector of nominal power injection setpoints.

C. Optimal Consensus-Based Frequency Control for Generator Models with Higher-Order Dynamics

Suppose the solution of the system (II.1) converges to a synchronous motion with $\omega^s = \mathbb{1}_n \omega^*$ and constants ω^*, P_m^s and P_s^s. Then, ω^* is obtained from

$$\mathbb{1}_n^\top M \dot{\omega}^s = \mathbb{1}_n^\top T_m \dot{P}_m^s = \mathbb{1}_n^\top T_s \dot{P}_s^s = 0$$

as

$$\omega^* = \frac{-\mathbb{1}_n^\top G V^2 + \mathbb{1}_n^\top P_m^d + \mathbb{1}_n^\top p^s}{\mathbb{1}_n^\top D \mathbb{1}_n + \mathbb{1}_n^\top K^{-1} \mathbb{1}_n},$$

where we have used the fact that $\mathbb{1}_n^\top \nabla U(\theta) = 0$. In practice, the load demand GV^2 is unknown and, hence, typically $-\mathbb{1}^\top G V^2 + \mathbb{1}_n^\top P_m^d \neq 0$. As a result, the synchronized frequency deviates from its nominal value. Thus, the main secondary control task is to restore the frequency to the nominal value via the inputs p.

Inspired by [9], [10], we consider the following consensus-based secondary frequency control scheme

$$T_p \dot{p} = -p + P_m - (I_n - K^{-1})\omega - A\mathcal{L}Ap, \qquad \text{(II.2)}$$

where $\mathcal{L} \in \mathbb{R}^{n \times n}$ is the Laplacian matrix of an undirected connected communication graph enabling distributed information exchange between the generators. Furthermore, the diagonal positive definite matrices $T_p \in \mathbb{R}^{n \times n}$ and $A = \text{diag}(A_{ii}) \in \mathbb{R}^{n \times n}$ denote the controller time constants and a weighting matrix, respectively. It follows from the analysis in [9], [10], that - if appropriately tuned - the control (II.2) is able to restore the frequency to its nominal value, while ensuring economic optimality in a synchronized state, i.e.,

$$A_{ii} p_i^s = A_{kk} p_k^s \quad \forall i \in \mathcal{N}, \quad \forall k \in \mathcal{N}.$$

Thus, usually the matrix A is fixed by economic considerations.

D. Communication Uncertainties: Time-Varying Delays and Dynamic Communication Network

The distributed nature of the protocol (II.2) requires nearest-neighbor information exchange, represented by the Laplacian matrix $\mathcal{L}$ in (II.2). Hence, as discussed in Section I, see also [13], [14], [22], communication uncertainties pose a serious threat to the power system performance. Therefore in the present paper we derive conditions under which the closed-loop power system dynamics are robust with respect to the practically most relevant communication uncertainties, namely message delays and information loss [13], [14].

Following [11], [21]–[23] we assume that a time-varying bounded communication delay $\tau_{ik} : \mathbb{R}_{\geq 0} \to [0, h_{ik}]$, $h_{ik} \in \mathbb{R}_{\geq 0}$, affects the information flow from node i to node k and that the control error e_{ik} is then computed as

$$e_{ik}(t) = A_{ii} p_i(t - \tau_{ik}(t)) - A_{kk} p_k(t - \tau_{ik}(t)).$$

Our analysis accounts for asymmetric delays, i.e., $\tau_{ik} \neq \tau_{ki}$. Furthermore, following standard practice in sampled-data and networked control systems [24], [25], the delay τ_{ik} can be piecewise-continuous in t and fast-varying, i.e., no restrictions on the existence, continuity, or boundedness of $\dot{\tau}_{ik}(t)$ are imposed. This characterization of the delay can be explained as follows. Assume that the control signal at the i-th node is generated by a zero-order hold function with bounded sampling interval $t_{i,\kappa+1} - t_{i,\kappa} \leq \bar{h}_i$, $\bar{h}_i \in \mathbb{R}_{>0}$, $\kappa \in \mathbb{Z}$. In addition, the control error generation e_{ik} is affected by a bounded, possibly time-varying, communication delay $\eta_{ik} : \mathbb{R}_{\geq 0} \to [0, \bar{\eta}_{ik}]$, $\bar{\eta}_{ik} \in \mathbb{R}_{\geq 0}$. Then we define

$$\tau_{ik}(t) = t - t_{i,\kappa} + \eta_{ik}(t) \leq \bar{h}_i + \bar{\eta}_{ik}, \quad t \in [t_{i,\kappa}, t_{i,\kappa+1}),$$

where $t_{i,\kappa} - \eta_{ik}$ is the time instant where the information is sampled and $t_{i,\kappa+1}$ is the time instant where the next input update arrives. Furthermore, $h_{ik} = \bar{h}_i + \bar{\eta}_{ik}$ is the assumed upper bound on τ_{ik} and $\dot{\tau}_{ik} = 1$.

The loss of information, e.g., due to package losses or link failures, is modeled via a dynamic communication network with switched communication topology $\mathcal{G}_\sigma(t)$ [21]–[23], [29]. Here, $\sigma : \mathbb{R}_{\geq 0} \to \mathcal{M}$ is a switching signal, $\mathcal{M} = \{1, 2, \ldots, \nu\}$, $\nu \in \mathbb{R}_{>0}$, is an index set and $\{\mathcal{G}_1, \mathcal{G}_2, \ldots, \mathcal{G}_\nu\}$ denotes the set of finite network topologies. We denote by $\mathcal{L}_\ell = \mathcal{L}(\mathcal{G}_\ell)$ the Laplacian matrix corresponding to the index $\ell = \sigma(t) \in \mathcal{M}$ and by $\mathcal{E}_\ell$ the corresponding set of edges. As done in [11], [21], [23], [29], we assume that the communication topology $\mathcal{G}_{\sigma(t)}$ is undirected and connected for all $t \in \mathbb{R}_{\geq 0}$. We also assume that the delays between two connected nodes are not affected by the switches in topology.

To derive the closed-loop system representation of (II.1) and (II.2) with communication uncertainties, we follow [11] and introduce the matrices $L_{\ell,m}$, $m = 1, \ldots, 2\bar{\mathcal{E}}$, $\bar{\mathcal{E}} = \max_{\ell = \sigma(t) \in \mathcal{M}} |\mathcal{E}_\ell|$, with nonzero entries $l_{\ell,m,ii} = 1$, $l_{\ell,m,ik} = -1$, if in the ℓ-th communication topology node i is connected to node k and all other entries are zero. Hence,

$$\mathcal{L}_\ell = \sum_{m=1}^{2\bar{\mathcal{E}}} L_{\ell,m}.$$

Furthermore, we define the vector $x = \text{col}(P_m, P_s, p) \in \mathbb{R}^{3n}$ as well as the matrices

$$T = \text{blkdiag}(T_m, T_s, T_p), \quad \bar{A} = \text{blkdiag}(A, A, A), \qquad \text{(II.3)}$$

$$\Phi = \begin{bmatrix} I_n & -I_n & \mathbb{0} \\ \mathbb{0} & I_n & -I_n \\ -I_n & \mathbb{0} & I_n \end{bmatrix} \qquad \text{(II.4)}$$

and

$$\Psi_{\ell,m} = \bar{A}\, \text{blkdiag}\left(\mathbb{0}, \mathbb{0}, L_{\ell,m}\right) \bar{A}. \qquad \text{(II.5)}$$

Then, by combining (II.1) with (II.2), the closed-loop dynamics with delays and dynamic communication network can be compactly written as

$$\begin{aligned} \dot{\theta} &= \omega, \\ M\dot{\omega} &= -D\omega - \nabla U(\theta) - GV^2 + P_m^d + \begin{bmatrix} I_n & \mathbb{0}_{n \times 2n} \end{bmatrix} x, \\ T\dot{x} &= -\Phi x - \left(\sum_{m=1}^{2\bar{\mathcal{E}}} \Psi_{\ell,m} x(t - \tau_m) \right) - \begin{bmatrix} \mathbb{0} \\ K^{-1} \\ I_n - K^{-1} \end{bmatrix} \omega. \end{aligned} \qquad \text{(II.6)}$$

Remark 2.1: The power system model employed in the related work [11] is derived under the assumptions that

$\|T_m\|_p \ll \|M\|_p$ and $\|T_s\|_p \ll \|M\|_p$, see also (II.3), where $\|\cdot\|_p$ denotes a matrix p-norm. Then, by invoking singular perturbation arguments the slow dynamics corresponding to the turbine-governor system in (II.6) can be represented by their corresponding steady-state equations [30], [31]. However, even though these parameter assumptions are prevalent in the control community, for many practical power plants they are not satisfied, see, e.g., the examples in [9], [15] and in Section IV. As a consequence, the turbine-governor dynamics are usually modeled explicitly in the related power systems literature on load frequency control [15]–[20]. These facts are the main motivation to extend the analysis in [11] to the model (II.6) in the present work. Due to the resulting higher-order dynamics different coordinate transformation and reduction steps than those employed in [11] are required to construct a *strict* LKF for the system (II.6). This problem is addressed in the next section.

III. Robust Stability in the Presence of Time-Varying Delays and Dynamic Communication Network

A. Coordinate Transformation and Reduction

We introduce both a coordinate transformation and reduction that are essential to construct the proposed strict LKF in Section III-C, which is used to establish our main stability result. This step is motivated by the following property of the matrix family

$$\Phi + \sum_{m=1}^{2\bar{\mathcal{E}}} \Psi_{\ell,m}, \quad \ell = \sigma(t) \in \mathcal{M},$$

which reveals an invariant subspace in the x-dynamics of the closed-loop power system model (II.6).

Lemma 3.1: Consider the matrices $\bar{A}$ in (II.3), Φ in (II.4) and $\Psi_{\ell,m}$ in (II.5). For any $v \in \mathbb{R}^{3n} \setminus \{\alpha \bar{A}^{-1}\mathbb{1}_{3n}\}$, $\alpha \in \mathbb{R}$,

$$v^\top \left(\frac{1}{2}\left(\Phi + \Phi^\top\right) + \sum_{m=1}^{2\bar{\mathcal{E}}} \Psi_{\ell,m} \right) v > 0. \tag{III.1}$$

Proof: To establish the claim, it is convenient to write the symmetric part of Φ as

$$\begin{bmatrix} \tilde{\Phi}_{11} & \tilde{\Phi}_{12} \\ * & I_n \end{bmatrix} = \frac{1}{2}\left(\Phi + \Phi^\top\right),$$

with

$$\tilde{\Phi}_{11} = \begin{bmatrix} I_n & -\frac{1}{2} I_n \\ -\frac{1}{2} I_n & I_n \end{bmatrix}, \qquad \tilde{\Phi}_{12} = -\frac{1}{2}\begin{bmatrix} I_n \\ I_n \end{bmatrix}.$$

Clearly, $\tilde{\Phi}_{11} > 0$ and

$$I_n - \tilde{\Phi}_{12}^\top \tilde{\Phi}_{11}^{-1} \tilde{\Phi}_{12} = \mathbb{0}.$$

Hence, the Schur complement implies that $\frac{1}{2}\left(\Phi + \Phi^\top\right) \geq 0$ and since $\tilde{\Phi}_{11} > 0$, in addition, we have that $v^\top \frac{1}{2}\left(\Phi + \Phi^\top\right) v > 0$ for all $v = \mathrm{col}(v_1, v_2, \mathbb{0}_n)$, $v_1 \in \mathbb{R}^n$, $v_2 \in \mathbb{R}^n$, $v \neq \mathbb{0}_{3n}$. Moreover, for any $\ell = \sigma(t) \in \mathcal{M}$, $\mathcal{L}_\ell$ is a Laplacian matrix of an undirected and connected graph. Hence,

$$v_3^\top A \mathcal{L}_\ell A v_3 > 0 \quad \forall\, v_3 \in \mathbb{R}^n \setminus \{\alpha A^{-1}\mathbb{1}_n\}, \quad \alpha \in \mathbb{R}.$$

The established facts imply that for any $\ell = \sigma(t) \in \mathcal{M}$, the matrix sum

$$\frac{1}{2}\left(\Phi + \Phi^\top\right) + \sum_{m=1}^{2\bar{\mathcal{E}}} \Psi_{\ell,m}$$

is positive semidefinite and that (III.1) is satisfied with equality if and only if $v_3 = \alpha A^{-1}\mathbb{1}_n$. In order for

$$\left(\frac{1}{2}\left(\Phi + \Phi^\top\right) + \sum_{m=1}^{2\bar{\mathcal{E}}} \Psi_{\ell,m} \right) v = \mathbb{0}_{3n}$$

to be satisfied for some $v = \mathrm{col}(v_1, v_2, v_3)$ with $v_3 = \alpha A^{-1}\mathbb{1}_n$, we see that v_1 and v_2 have to satisfy

$$\begin{aligned} v_1 - \frac{1}{2}v_2 - \alpha\frac{1}{2}A^{-1}\mathbb{1}_n &= \mathbb{0}_n, \\ -\frac{1}{2}v_1 + v_2 - \alpha\frac{1}{2}A^{-1}\mathbb{1}_n &= \mathbb{0}_n, \\ -\frac{1}{2}v_1 - \frac{1}{2}v_2 + \alpha A^{-1}\mathbb{1}_n &= \mathbb{0}_n. \end{aligned}$$

By using the second equation, we can express v_2 as

$$v_2 = \frac{1}{2}v_1 + \alpha\frac{1}{2}A^{-1}\mathbb{1}_n.$$

Moreover, by substituting the value of v_2 in the third equation, we obtain $v_1 = \alpha A^{-1}\mathbb{1}_n$, which gives $v_2 = \alpha A^{-1}\mathbb{1}_n$, completing the proof. ∎

In light of Lemma 3.1 and inspired by [11], [21], [29], consider the change of coordinates

$$\begin{bmatrix} \bar{x} \\ \zeta \end{bmatrix} = \mathcal{W}^\top T^{\frac{1}{2}} x, \quad \mathcal{W} = \begin{bmatrix} W & \frac{1}{\sqrt{\mu}} T^{\frac{1}{2}} \bar{A}^{-1}\mathbb{1}_{3n} \end{bmatrix}, \tag{III.2}$$

where $W \in \mathbb{R}^{3n \times 3n-1}$, $\bar{A}$ is given in (II.3), $\mu = \|T^{\frac{1}{2}}\bar{A}^{-1}\mathbb{1}_{3n}\|_2^2$, W is chosen such that $W^\top T^{\frac{1}{2}}\bar{A}^{-1}\mathbb{1}_{3n} = \mathbb{0}_{3n-1}$ and the transformation matrix $\mathcal{W} \in \mathbb{R}^{3n\times 3n}$ is orthogonal, i.e., $\mathcal{W}\mathcal{W}^\top = I_{3n}$. Thus, $\bar{x}$ is a projection of x on the subspace orthogonal to $T^{\frac{1}{2}}\bar{A}^{-1}\mathbb{1}_{3n}$ scaled by $T^{\frac{1}{2}}$.

From (III.2) we have that

$$\zeta(x) = \frac{1}{\sqrt{\mu}}\mathbb{1}_{3n}^\top \bar{A}^{-1} T^{\frac{1}{2}} T^{\frac{1}{2}} x = \frac{1}{\sqrt{\mu}}\mathbb{1}_{3n}^\top \bar{A}^{-1} T x. \tag{III.3}$$

Using (II.6) together with the fact $\mathbb{1}_{3n}^\top \bar{A}^{-1}\Phi_{\ell,m} = \mathbb{0}_{3n}$ leads to

$$\dot{\zeta}(x) = \frac{1}{\sqrt{\mu}}\mathbb{1}_{3n}^\top \bar{A}^{-1} T \dot{x} = -\frac{1}{\sqrt{\mu}}\mathbb{1}_n^\top A^{-1}\omega,$$

which by integrating with respect to time and recalling (II.6) and (III.3) yields

$$\zeta(x) = -\frac{1}{\sqrt{\mu}}\mathbb{1}_n^\top A^{-1}\theta + \zeta_0, \tag{III.4}$$

where we have defined

$$\zeta_0 = \frac{1}{\sqrt{\mu}}\mathbb{1}_n^\top A^{-1}\theta_0 + \frac{1}{\sqrt{\mu}}\mathbb{1}_{3n}^\top \bar{A}^{-1} T x_0.$$

Furthermore,

$$x = T^{-\frac{1}{2}}\mathcal{W}\begin{bmatrix}\bar{x}\\ \zeta\end{bmatrix} = T^{-\frac{1}{2}}W\bar{x} - \frac{1}{\mu}\bar{A}^{-1}\mathbb{1}_{3n}\left(\mathbb{1}_n^\top A^{-1}\theta - \mu\zeta_0\right).$$

Hence,

$$\begin{aligned}\dot{\tilde{x}} &= W^\top T^{\frac{1}{2}}\dot{x} = -W^\top T^{-\frac{1}{2}}\Phi T^{-\frac{1}{2}}W\bar{x}\\ &\quad - W^\top T^{-\frac{1}{2}}\left(\sum_{m=1}^{2\bar{\mathcal{E}}}\Psi_{\ell,m}T^{-\frac{1}{2}}W\bar{x}(t-\tau_m)\right)\\ &\quad - W^\top T^{-\frac{1}{2}}\begin{bmatrix}\mathbb{0}\\ K^{-1}\\ I_n - K^{-1}\end{bmatrix}\omega,\end{aligned}$$

where we have used the facts that $\Phi\bar{A}^{-1}\mathbb{1}_{3n} = \mathbb{0}_{3n}$ and $\Psi_{\ell,m}\bar{A}^{-1}\mathbb{1}_{3n} = \mathbb{0}_{3n}$.

By substituting ζ by (III.4), the overall closed loop system (II.6) can be expressed in the reduced order coordinates as

$$\begin{aligned}\dot{\theta} &= \omega,\\ M\dot{\omega} &= -D\omega - \nabla U(\theta) - GV^2 + P_m^d + \begin{bmatrix}I_n & \mathbb{0}_{n\times 2n}\end{bmatrix}T^{-\frac{1}{2}}W\bar{x}\\ &\quad - \frac{1}{\mu}A^{-1}\mathbb{1}_n(\mathbb{1}_n{}^\top A^{-1}\theta - \mu\zeta_0),\\ \dot{\tilde{x}} &= -W^\top T^{-\frac{1}{2}}\Phi T^{-\frac{1}{2}}W\bar{x} - W^\top T^{-\frac{1}{2}}\begin{bmatrix}\mathbb{0}\\ K^{-1}\\ I_n - K^{-1}\end{bmatrix}\omega\\ &\quad - W^\top T^{-\frac{1}{2}}\left(\sum_{m=1}^{2\bar{\mathcal{E}}}\Psi_{\ell,m}T^{-\frac{1}{2}}W\bar{x}(t-\tau_m)\right).\end{aligned} \tag{III.5}$$

B. Error system

We make the following standard assumption on existence of an equilibrium point satisfying the usual security constraint on the stationary phase angle differences [9]–[11].

Assumption 3.2: The system (III.5) possesses an equilibrium point $\text{col}(\theta^s, \mathbb{0}_n, \bar{x}^s) \in \mathbb{R}^{5n-1}$, such that

$$|\theta_i^s - \theta_k^s| < \frac{\pi}{2} \quad \forall i \in \mathcal{N},\ \forall k \in \mathcal{N}_i.$$

With Assumption 3.2, we define the error states

$$\tilde{\theta} = \theta - \theta^s, \quad \tilde{x} = \bar{x} - \bar{x}^s, \quad z = \text{col}(\tilde{\theta}, \omega, \tilde{x}) \in \mathbb{R}^{5n-1}.$$

The dynamics (III.5) expressed in the error coordinates are given by

$$\begin{aligned}\dot{\tilde{\theta}} &= \omega,\\ M\dot{\omega} &= -D\omega - \nabla U(\tilde{\theta}+\theta^s) + \nabla U(\theta^s) + \begin{bmatrix}I_n & \mathbb{0}_{n\times 2n}\end{bmatrix}T^{-\frac{1}{2}}W\tilde{x}\\ &\quad - \frac{1}{\mu}A^{-1}\mathbb{1}_n^\top\mathbb{1}_n A^{-1}\tilde{\theta},\\ \dot{\tilde{x}} &= -W^\top T^{-\frac{1}{2}}\Phi T^{-\frac{1}{2}}W\tilde{x} - W^\top T^{-\frac{1}{2}}\begin{bmatrix}\mathbb{0}\\ K^{-1}\\ I_n - K^{-1}\end{bmatrix}\omega\\ &\quad - W^\top T^{-\frac{1}{2}}\left(\sum_{m=1}^{2\bar{\mathcal{E}}}\Psi_{\ell,m}T^{-\frac{1}{2}}W\tilde{x}(t-\tau_m)\right).\end{aligned} \tag{III.6}$$

Clearly, with Assumption 3.2, the system (III.6) has an equilibrium point z^s at the origin. Furthermore, asymptotic stability of z^s implies that any solution $\text{col}(\theta, \omega, x)$ of the original system (II.6) with an initial condition that satisfies

$$\zeta_0 = \frac{1}{\sqrt{\mu}}\mathbb{1}_n^\top A^{-1}\theta_0 + \frac{1}{\sqrt{\mu}}\mathbb{1}_{3n}^\top\bar{A}^{-1}Tx_0$$

converges to an equilibrium $\text{col}(\theta^s, \mathbb{0}_n, x^s)$. This applies for any value of ζ_0. Moreover, the dynamics in (III.6) are independent of ζ. Consequently, z^s being asymptotically stable implies that all solutions of the original system (II.6) converge to an equilibrium point.

C. Main Result

To present our main result, it is convenient to define the following two matrices

$$\bar{\Phi} = W^\top T^{-\frac{1}{2}}\Phi T^{-\frac{1}{2}}W, \tag{III.7}$$

$$\bar{\Psi}_{\ell,m} = W^\top T^{-\frac{1}{2}}\Psi_{\ell,m}T^{-\frac{1}{2}}W. \tag{III.8}$$

Note that Lemma 3.1 implies that $\bar{\Phi} + \sum_{m=1}^{2\bar{\mathcal{E}}}\bar{\Psi}_{\ell,m} > 0$, which is essential to derive a strict LKF for the dynamics (III.6) and, thus, establish the result below.

Proposition 3.3: Consider the system (III.6) with Assumption 3.2. Fix A, K, $\mathcal{L}$, T and D as well as $h_m \in \mathbb{R}_{>0}$, $m = 1, \ldots, 2\bar{\mathcal{E}}$. Suppose that for all $\Psi_{\ell,m}$ defined in (III.8), $\ell = 1, \ldots, |\mathcal{M}|$, there exist matrices $R_m > 0 \in \mathbb{R}^{(3n-1)\times(3n-1)}$, $S_m > 0 \in \mathbb{R}^{(3n-1)\times(3n-1)}$, $P > 0 \in \mathbb{R}^{(3n-1)\times(3n-1)}$, $P_2 \in \mathbb{R}^{(3n-1)\times(3n-1)}$, $P_3 > 0 \in \mathbb{R}^{(3n-1)\times(3n-1)}$, and $S_{12,m} \in \mathbb{R}^{(3n-1)\times(3n-1)}$ satisfying

$$\mathcal{Q} = \begin{bmatrix}-D & \mathcal{Q}_{12} & \mathcal{Q}_{13} & \mathbb{0}_{n\times(3n-1)} & \mathbb{0}_{n\times(3n-1)}\\ * & \mathcal{Q}_{22} & \mathcal{Q}_{23} & S_{12} & \mathcal{Q}_{25}\\ * & * & \mathcal{Q}_{33} & \mathbb{0} & \mathcal{Q}_{35}\\ * & * & * & -S-R & R - S_{12}^\top\\ * & * & * & * & \mathcal{Q}_{55}\end{bmatrix} < 0, \tag{III.9}$$

where

$$\begin{aligned}&R = \text{blockdiag}(R_m),\ S = \text{blockdiag}(S_m),\\ &S_{12} = \text{blockdiag}(S_{12,m}),\\ &\mathcal{Q}_{12} = \frac{1}{2}\begin{bmatrix}I_n & \mathbb{0}_{n\times 2n}\end{bmatrix}T^{-\frac{1}{2}}W\\ &\qquad - \begin{bmatrix}\mathbb{0} & K^{-1} & I_n - K^{-1}\end{bmatrix}T^{-\frac{1}{2}}WP_2,\\ &\mathcal{Q}_{13} = -\begin{bmatrix}\mathbb{0} & K^{-1} & I_n - K^{-1}\end{bmatrix}T^{-\frac{1}{2}}WP_3,\\ &\mathcal{Q}_{22} = -P_2^\top\bar{\Phi} - \bar{\Phi}^\top P_2 + \sum_{k=1}^{2\bar{\mathcal{E}}}S_k - \sum_{k=1}^{2\bar{\mathcal{E}}}R_k,\\ &\mathcal{Q}_{23} = -\bar{\Phi}^\top P_3 + P - P_2^\top, \quad \mathcal{Q}_{25} = \begin{bmatrix}\bar{\mathcal{Q}}_{25,1} \ldots \bar{\mathcal{Q}}_{25,2\bar{\mathcal{E}}}\end{bmatrix},\\ &\bar{\mathcal{Q}}_{25,m} = R_m - S_{12,m} - P_2^\top\bar{\Psi}_{\ell,m},\\ &\mathcal{Q}_{33} = -P_3 - P_3^\top + \sum_{k=1}^{2\bar{\mathcal{E}}}h_k^2R_k,\ \mathcal{Q}_{35} = \begin{bmatrix}\bar{\mathcal{Q}}_{35,1} \ldots \bar{\mathcal{Q}}_{35,2\bar{\mathcal{E}}}\end{bmatrix},\\ &\bar{\mathcal{Q}}_{35,m} = -P_3^\top\bar{\Psi}_{\ell,m}, \qquad \mathcal{Q}_{55} = -2R + S_{12} + S_{12}^\top\end{aligned}$$

as well as

$$\begin{bmatrix} R & S_{12} \\ * & R \end{bmatrix} \geq 0. \tag{III.10}$$

Then, for all $\tau_m(t) \in [0, h_m]$ the origin is a locally uniformly asymptotically stable equilibrium point of the system (III.6).

Proof: By noting that the delay only appears in $\tilde{x}$ and inspired by [9], [11], [25] consider the LKF with $\epsilon \in \mathbb{R}_{>0}$,

$$\begin{aligned} V &= V_1 + \sum_{m=1}^{2\bar{\mathcal{E}}} V_{2m}, \\ V_1 &= \frac{1}{2}\omega^\top M\omega + U(\tilde{\theta}+\theta^s) - \nabla U(\theta^s)^\top\tilde{\theta} \\ &\quad + \tilde{x}^\top P\tilde{x} + \epsilon\omega^\top M\mathbb{1}_n\mathbb{1}_n^\top A^{-1}\tilde{\theta} + \frac{1}{2\mu}(\mathbb{1}_n^\top A^{-1}\tilde{\theta})^2 \\ &\quad + \epsilon\omega^\top AM\left(\nabla U(\tilde{\theta}+\theta^s) - \nabla U(\theta^s)\right), \\ V_{2m} &= \int_{t-h_m}^{t} \tilde{x}^\top(s) S_m \tilde{x}(s) ds \\ &\quad + h_m \int_{-h_m}^{0}\int_{t+\phi}^{t} \dot{\tilde{x}}^\top(s) R_m \dot{\tilde{x}}(s) ds d\phi. \end{aligned} \tag{III.11}$$

To establish the claim, we first show that the above LKF is locally positive definite. We have that

$$\nabla V_1 = \begin{bmatrix} \nabla v_1 \\ \nabla v_2 \\ 2P\tilde{x} \end{bmatrix},$$

where

$$\begin{aligned} \nabla v_1 &= \nabla U(\tilde{\theta}+\theta^s) - \nabla U(\theta^s) + \epsilon\nabla^2 U(\tilde{\theta}+\theta^s)^\top MA\omega \\ &\quad + \frac{1}{\mu}(A^{-1}\mathbb{1}_n\mathbb{1}_n^\top A^{-1})\tilde{\theta} + \epsilon A^{-1}\mathbb{1}_n\mathbb{1}_n^\top M\omega, \\ \nabla v_2 &= M\omega + \epsilon AM(\nabla U(\tilde{\theta}+\theta^s) - \nabla U(\theta^s)) \\ &\quad + \epsilon M\mathbb{1}_n\mathbb{1}_n^\top A^{-1}\tilde{\theta}. \end{aligned}$$

Clearly, at the origin $\nabla V_1|_{z^s} = \mathbb{0}_{5n-1}$. Moreover the Hessian of V_1 evaluated at z^s is given by

$$\nabla^2 V_1|_{z^s} = \begin{bmatrix} \nabla^2 v_{11} & \nabla^2 v_{12} & \mathbb{0}_{n\times(3n-1)} \\ * & M & \mathbb{0}_{n\times(3n-1)} \\ * & * & 2P \end{bmatrix},$$

where

$$\begin{aligned} \nabla^2 v_{11} &= \nabla^2 U(\theta^s) + \frac{1}{\mu}A^{-1}\mathbb{1}_n\mathbb{1}_n^\top A^{-1}, \\ \nabla^2 v_{12} &= \epsilon AM\nabla^2 U(\theta^s) + \epsilon M\mathbb{1}_n\mathbb{1}_n^\top A^{-1}. \end{aligned}$$

It is well-known that $\nabla^2 U(\theta^s)$ is a Laplacian matrix with $\ker(\nabla^2 U(\theta^s)) = \text{span}(\mathbb{1}_n)$ [32], [33]. Furthermore, $A^{-1}\mathbb{1}_n\mathbb{1}_n^\top A^{-1}$ is a positive semidefinite matrix and $\ker(A^{-1}\mathbb{1}_n\mathbb{1}_n^\top A^{-1}) \cap \ker(\nabla^2 U(\theta^s)) = \mathbb{0}_n$. In addition, M is a diagonal matrix with positive diagonal entries and P is a positive definite matrix. Thus, all block-diagonal entries of $\nabla^2 V_1|_{z^s}$ are positive definite. This implies that there is a sufficiently small $\epsilon^s > 0$ such that for all $\epsilon \in]0, \epsilon^s]$ we have that $\nabla^2 V_1|_{z^s} > 0$. Furthermore, S_m and R_m in V_{2m} are positive definite matrices. Therefore, z^s is a strict minimum of V.

Following [12], [25], at first we set $\epsilon = 0$ in (III.11). Then the time derivatives of V_1 and V_{2m} are given by

$$\begin{aligned} \dot{V}_1 &= -\omega^\top D\omega + \omega^\top \begin{bmatrix} I_n & \mathbb{0}_{n\times 2n} \end{bmatrix} T^{-\frac{1}{2}} W\tilde{x} + 2\dot{\tilde{x}}^\top P\tilde{x} \\ \dot{V}_{2m} &= \tilde{x}^\top S_m\tilde{x} - \tilde{x}^\top(t-h_m)S_m\tilde{x}(t-h_m) \\ &\quad + h_m^2\dot{\tilde{x}}^\top R_m\dot{\tilde{x}} - h_m\int_{t-h_m}^{t}\dot{\tilde{x}}^\top(s)R_m\dot{\tilde{x}}(s)ds. \end{aligned} \tag{III.12}$$

Furthermore, since (III.10) is satisfied by assumption, applying Jensen's inequality together with [25, Lemma 3.3] yields

$$-h_m\int_{t-h_m}^{t}\dot{\tilde{x}}(s)^\top R_m\dot{\tilde{x}}(s)ds \leq -\eta_m^\top\begin{bmatrix} R_m & S_{12,m} \\ * & R_m \end{bmatrix}\eta_m, \tag{III.13}$$

where $\eta_m = \text{col}(\tilde{x} - \tilde{x}(t-\tau_m), \tilde{x}(t-\tau_m) - \tilde{x}(t-h_m))$ Next, we apply the descriptor method, see [25, Chapter 3], i.e., we introduce

$$\begin{aligned} 0 &= 2\left[\tilde{x}^\top P_2^\top + \dot{\tilde{x}}^\top P_3^\top\right] \\ &\quad \left[-W^\top T^{-\frac{1}{2}}\begin{bmatrix} \mathbb{0} \\ K^{-1} \\ I_n - K^{-1} \end{bmatrix}\omega - W^\top T^{-\frac{1}{2}}\Phi T^{-\frac{1}{2}}W\tilde{x}\right. \\ &\quad \left. -W^\top T^{-\frac{1}{2}}\left(\sum_{m=1}^{2\bar{\mathcal{E}}}\Psi_{\ell,m}T^{-\frac{1}{2}}W\tilde{x}(t-\tau_m)\right) - \dot{\tilde{x}}\right]. \end{aligned} \tag{III.14}$$

By summing over (III.13), adding (III.14) together with (III.12), and recalling $\bar{\Phi}$ in (III.7) and $\bar{\Psi}_{\ell,m}$ in (III.8), we obtain

$$\dot{V} \leq \xi^\top \mathcal{Q}\xi,$$

where

$$\begin{aligned} \xi &= \text{col}\left(\omega, \tilde{x}, \dot{\tilde{x}}, \xi_1, \xi_2\right), \\ \xi_1 &= \text{col}\left(\tilde{x}(t-h_1), \ldots, \tilde{x}(t-h_{2\bar{\mathcal{E}}})\right), \\ \xi_2 &= \text{col}\left(\tilde{x}(t-\tau_1), \ldots, \tilde{x}(t-\tau_{2\bar{\mathcal{E}}})\right), \end{aligned}$$

and $\mathcal{Q}$ is defined in (III.9).

Note that for $\epsilon = 0$ the time derivative of the LKF is not strict. Yet, under the standing assumptions, $\mathcal{Q} < 0$. Hence, for $\epsilon \neq 0$, $\dot{V}$ can be strictified in a straightforward manner following [11, Proposition 7]. Thus,

$$\dot{V} \leq -\nu\left(\|x\|_2^2\right)$$

for some (sufficiently small) $\epsilon \in \mathbb{R}_{>0}$ and $\nu \in \mathbb{R}_{>0}$. By invoking [25, Lemma 4.3] we conclude that the origin of the system (III.6) is locally uniformly asymptotically stable. ■

IV. Numerical Example

The efficacy of the stability condition in Proposition 3.3 is evaluated via a benchmark example based on Kundur's four-machine-two-area test system [2], see Fig. 1. This example has also been used in [11], where a related analysis is conducted for a power system model in which the generator

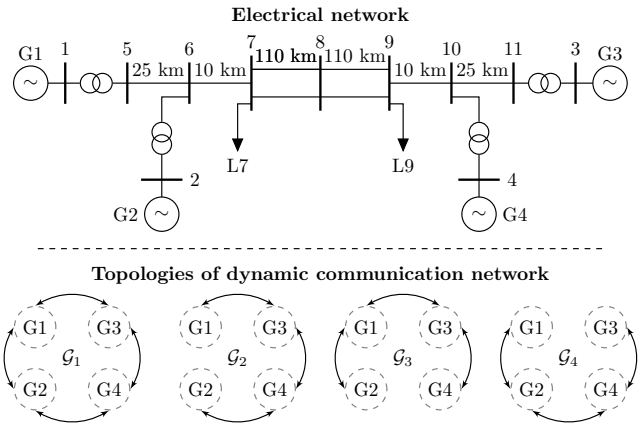

Fig. 1. Kundur's two-area-four-machine test system taken from [2, Example 12.6] and the four employed topologies of the switched communication network.

dynamics are solely represented by the swing equation. The model used in [11] can be obtained from (II.6) by setting $T_m\dot{P}_m = T_s\dot{P}_s = \mathbb{0}_n$ for all $t \geq 0$, which yields

$$\begin{aligned} P_m &= -K^{-1}\omega + p, \\ T_p\dot{p} &= -I_n\omega - \sum_{m=1}^{2\bar{\mathcal{E}}} AL_{\ell,m}Ap(t-\tau_m), \end{aligned} \tag{IV.1}$$

with angle and frequency dynamics as in (II.6).

The values of the main system parameters are given in [2] with $M = \text{diag}(13.00, 13.00, 12.35, 12.35)$. The following modifications are made: we assume damping coefficients $D_i = 2.3$ pu and droop gains $K_i = 0.05$ pu (with respect to the rated machine powers $S_{G,i} = [700, 700, 719, 700]$, $i = 1, \ldots, 4$). Also, we introduce the steam turbine as well as the governor time constants $T_m = \text{diag}(0.125, 0.1, 0.125, 0.11)$ and $T_s = \text{diag}(3.6, 1.8, 2.25, 4.5)$. Clearly, the assumption $\|T_s\|_p \ll \|M\|_p$ is not satisfied, see Remark 2.1. We remark that in the literature values for $T_{s,i}$ and $T_{m,i}$ up to $5-10$ s are reported [15], [19].

With regard to the communication uncertainties, we consider four different communication topologies, see Fig. 1. Furthermore, we consider uniform fast-varying delays $\tau_m(t) = \tau(t)$ with $\tau(t) \leq h = 0.5$ s in (II.6). This delay is implemented as a piecewise continuous function with 2 ms sampling time. We compare the performance of the stability conditions given in Proposition 3.3 for the higher-order power system model (II.6) with those derived in [11] for the reduced-order model (IV.1). To this end, as in [11], we set $T_p = \frac{1}{0.05\kappa}A$, where $\kappa > 0$ is a free tuning parameter. For the given h, the maximum κ obtained via the stability conditions provided in [11] is $\bar{\kappa} = 16.0678$. Compared to this, the conditions of Proposition 3.3 are satisfied for $\hat{\kappa} = 0.902\bar{\kappa} = 14.4932$. This shows that the conditions of Proposition 3.3 do not introduce significant restrictions with regard to the admissible feedback gain, while they have the additional benefit of also guaranteeing stability in the presence of (non-passive) higher-order turbine-governor dynamics. Note that, even without delays

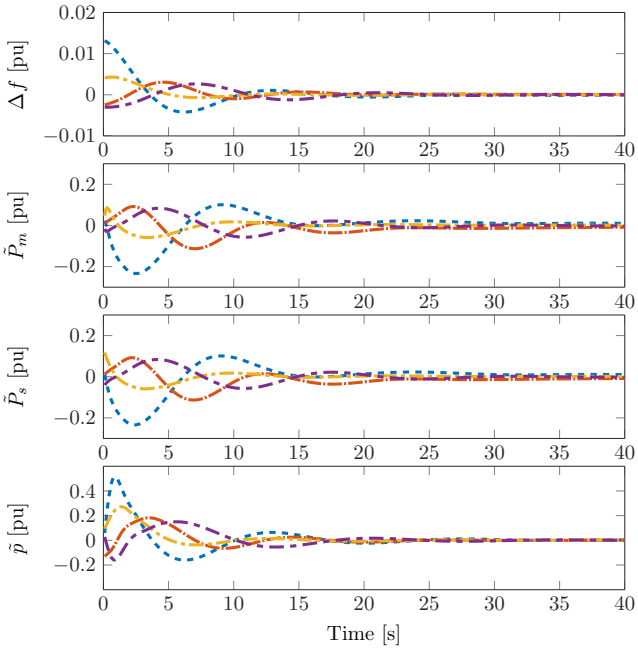

Fig. 2. Simulation results with $\kappa = 14.4932$, $h = 0.5s$.

or a switched communication network, disregarding these higher-order dynamics can lead to instability, see, e.g., the example in [9].

The analysis is further confirmed in simulation. The results in Fig. 2 show that the system trajectories converge to an equilibrium point for $\kappa = 14.4932$ with $\tau \leq 0.5$ s and the communication topologies are randomly switched every 5 s. Thus, despite the presence of communication uncertainties, the secondary frequency control objectives are achieved.

V. Conclusions

We have performed a robust stability analysis for a power system model with distributed consensus-based frequency control considering (non-passive) second-order turbine-governor dynamics as well as heterogeneous fast-varying delays and time-varying communication topologies. The analysis was conducted by introducing a novel coordinate transformation, which is instrumental to subsequently construct a strict LKF for the closed-loop power system dynamics. The efficacy of the derived conditions has been illustrated via a numerical example.

In future work, we will extend the analysis to more generic higher-order generator models and also consider other types of distributed secondary frequency controllers, e.g., primal-dual variants [3]–[5]. Furthermore, we plan to evaluate the performance of our stability criterion on large-scale power system models and derive tuning criteria for the controller gains.

References

[1] H. Farhangi, "The path of the smart grid," *IEEE Power and Energy Magazine*, vol. 8, no. 1, pp. 18 –28, january-february 2010.
[2] P. Kundur, *Power system stability and control*. McGraw-Hill, 1994.

[3] T. Stegink, C. De Persis, and A. van der Schaft, "A unifying energy-based approach to stability of power grids with market dynamics," *IEEE Transactions on Automatic Control*, vol. 62, no. 6, pp. 2612–2622, 2017.

[4] N. Li, C. Zhao, and L. Chen, "Connecting automatic generation control and economic dispatch from an optimization view," *IEEE Transactions on Control of Network Systems*, vol. 3, no. 3, pp. 254–264, 2016.

[5] L. Chen and S. You, "Reverse and forward engineering of frequency control in power networks," *IEEE Transactions on Automatic Control*, vol. 62, no. 9, pp. 4631–4638, 2017.

[6] S. Trip, M. Bürger, and C. D. Persis, "An internal model approach to (optimal) frequency regulation in power grids with time-varying voltages," *Automatica*, vol. 64, pp. 240 – 253, 2016.

[7] F. Dörfler, J. W. Simpson-Porco, and F. Bullo, "Breaking the hierarchy: Distributed control and economic optimality in microgrids," *IEEE Transactions on Control of Network Systems*, vol. 3, no. 3, pp. 241–253, 2016.

[8] J. Schiffer and F. Dörfler, "On stability of a distributed averaging PI frequency and active power controlled differential-algebraic power system model," in *Control Conference (ECC), 2016 European*. IEEE, 2016, pp. 1487–1492.

[9] S. Trip and C. D. Persis, "Distributed optimal load frequency control with non-passive dynamics," *IEEE Transactions on Control of Network Systems*, vol. PP, no. 99, pp. 1–1, 2017.

[10] A. Kasis, N. Monshizadeh, and I. Lestas, "A novel distributed secondary frequency control scheme for power networks with high order turbine governor dynamics," in *European Control Conference*, 2018.

[11] J. Schiffer, F. Dörfler, and E. Fridman, "Robustness of distributed averaging control in power systems: Time delays & dynamic communication topology," *Automatica*, vol. 80, pp. 261–271, 2017.

[12] S. Alghamdi, J. Schiffer, and E. Fridman, "Distributed secondary frequency control design for microgrids: Trading off L_2-gain performance and communication efforts under time-varying delays," in *European Control Conference*, 2018.

[13] G. Strbac, N. Hatziargyriou, J. P. Lopes, C. Moreira, A. Dimeas, and D. Papadaskalopoulos, "Microgrids: Enhancing the resilience of the European megagrid," *IEEE Power and Energy Magazine*, vol. 13, no. 3, pp. 35–43, 2015.

[14] Q. Yang, J. A. Barria, and T. C. Green, "Communication infrastructures for distributed control of power distribution networks," *IEEE Transactions on Industrial Informatics*, vol. 7, no. 2, pp. 316–327, 2011.

[15] C. K. Zhang, L. Jiang, Q. H. Wu, Y. He, and M. Wu, "Delay-dependent robust load frequency control for time delay power systems," *IEEE Transactions on Power Systems*, vol. 28, no. 3, pp. 2192–2201, Aug 2013.

[16] N. Chuang, "Robust H^∞ load-frequency control in interconnected power systems," *IET Control Theory Applications*, vol. 10, no. 1, pp. 67–75, 2016.

[17] H. Bevrani and T. Hiyama, "A control strategy for LFC design with communication delays," in *2005 International Power Engineering Conference*, Nov 2005, pp. 1087–1092 Vol. 2.

[18] W. Tan and Z. Xu, "Robust analysis and design of load frequency controller for power systems," *Electric Power Systems Research*, vol. 79, no. 5, pp. 846 – 853, 2009.

[19] A. N. Venkat, I. A. Hiskens, J. B. Rawlings, and S. J. Wright, "Distributed MPC strategies with application to power system automatic generation control," *IEEE Transactions on Control Systems Technology*, vol. 16, no. 6, pp. 1192–1206, Nov 2008.

[20] H. Bevrani and T. Hiyama, "On load-frequency regulation with time delays: Design and real-time implementation," *IEEE Transactions on Energy Conversion*, vol. 24, no. 1, pp. 292–300, March 2009.

[21] R. Olfati-Saber and R. M. Murray, "Consensus problems in networks of agents with switching topology and time-delays," *IEEE Transactions on Automatic Control*, vol. 49, no. 9, pp. 1520–1533, 2004.

[22] J. P. Hespanha, P. Naghshtabrizi, and Y. Xu, "A survey of recent results in networked control systems," *Proceedings of the IEEE*, vol. 95, no. 1, pp. 138–162, 2007.

[23] R. Olfati-Saber, J. A. Fax, and R. M. Murray, "Consensus and cooperation in networked multi-agent systems," *Proceedings of the IEEE*, vol. 95, no. 1, pp. 215–233, 2007.

[24] E. Fridman, "Tutorial on Lyapunov-based methods for time-delay systems," *European Journal of Control*, vol. 20, no. 6, pp. 271–283, 2014.

[25] ——, *Introduction to time-delay systems: analysis and control*. Birkhäuser, 2014.

[26] C. Godsil and G. Royle, *Algebraic Graph Theory*. Springer, 2001.

[27] R. Diestel, *Graduate texts in mathematics: Graph theory*. Springer, 2000.

[28] P. Sauer and M. Pai, *Power system dynamics and stability*. Prentice Hall, 1998.

[29] P. Lin and Y. Jia, "Average consensus in networks of multi-agents with both switching topology and coupling time-delay," *Physica A: Statistical Mechanics and its Applications*, vol. 387, no. 1, pp. 303–313, 2008.

[30] V. Venkatasubramanian, H. Schattler, and J. Zaborszky, "Fast time-varying phasor analysis in the balanced three-phase large electric power system," *IEEE Transactions on Automatic Control*, vol. 40, no. 11, pp. 1975–1982, 1995.

[31] J. Schiffer, D. Zonetti, R. Ortega, A. M. Stanković, T. Sezi, and J. Raisch, "A survey on modeling of microgrids—from fundamental physics to phasors and voltage sources," *Automatica*, vol. 74, pp. 135–150, 2016.

[32] J. W. Simpson-Porco, F. Dörfler, and F. Bullo, "Synchronization and power sharing for droop-controlled inverters in islanded microgrids," *Automatica*, vol. 49, no. 9, pp. 2603 – 2611, 2013.

[33] J. Schiffer, R. Ortega, A. Astolfi, J. Raisch, and T. Sezi, "Conditions for stability of droop-controlled inverter-based microgrids," *Automatica*, vol. 50, no. 10, pp. 2457–2469, 2014.